THE FASEB JOURNAL • RESEARCH • www.fasebj.org

Pharmacologic activation of estrogen receptor β increases mitochondrial function, energy expenditure, and brown adipose tissue

Suriyan Ponnusamy,[*] Quynh T. Tran,[†] Innocence Harvey,[‡] Heather S. Smallwood,[§] Thirumagal Thiyagarajan,[*] Souvik Banerjee,[¶] Daniel L. Johnson,[‖] James T. Dalton,[#,1] Ryan D. Sullivan,[**] Duane D. Miller,[¶] Dave Bridges,[‡,§,2] and Ramesh Narayanan[*,††,3]

[*]Department of Medicine, [†]Department of Preventive Medicine, [‡]Department of Physiology, [§]Department of Pediatrics, [¶]Department of Pharmaceutical Sciences, [‖]Molecular Informatics Core, and [**]Department of Comparative Medicine, University of Tennessee Health Science Center, Memphis, Tennessee, USA; [#]Preclinical Research and Development, GTx, Incorporated, Memphis, Tennessee, USA; and [††]West Cancer Center, Memphis, Tennessee, USA

ABSTRACT: Most satiety-inducing obesity therapeutics, despite modest efficacy, have safety concerns that underscore the need for effective peripherally acting drugs. An attractive therapeutic approach for obesity is to optimize/maximize energy expenditure by increasing energy-utilizing thermogenic brown adipose tissue. We used *in vivo* and *in vitro* models to determine the role of estrogen receptor β (ER-β) and its ligands on adipose biology. RNA sequencing and metabolomics were used to determine the mechanism of action of ER-β and its ligands. Estrogen receptor β (ER-β) and its selective ligand reprogrammed preadipocytes and precursor stem cells into brown adipose tissue and increased mitochondrial respiration. An ER-β-selective ligand increased markers of tricarboxylic acid–dependent and –independent energy biogenesis and oxygen consumption in mice without a concomitant increase in physical activity or food consumption, all culminating in significantly reduced weight gain and adiposity. The antiobesity effects of ER-β ligand were not observed in ER-β-knockout mice. Serum metabolite profiles of adult lean and juvenile mice were comparable, while that of adult obese mice was distinct, indicating a possible impact of obesity on age-dependent metabolism. This phenotype was partially reversed by ER-β-selective ligand. These data highlight a new role for ER-β in adipose biology and its potential to be a safer alternative peripheral therapeutic target for obesity.—Ponnusamy, S., Tran, Q. T., Harvey, I., Smallwood, H. S., Thiyagarajan, T., Banerjee, S., Johnson, D. L., Dalton, J. T., Sullivan, R. D., Miller, D. D., Bridges, D., Narayanan, R. Pharmacologic activation of estrogen receptor β increases mitochondrial function, energy expenditure, and brown adipose tissue. FASEB J. 31, 266–281 (2017). www.fasebj.org

KEY WORDS: exercise mimetic · mitochondria · oxygen consumption · obesity · metabolic diseases

Obesity is pandemic, with over 50% of the global population and two-thirds of the U.S. population overweight or obese (1, 2). Obesity is a serious health risk factor: it is directly associated with numerous comorbidities (3, 4) and is correlated with an increased associated mortality rate (5). The obesity epidemic also has significant economic consequences. A forecast suggests that if the 12.7 million obese children living today in the United States remain overweight throughout their life, it will result in a cost to economy of $1.1 trillion, or 6% of the U.S. gross domestic product (6).

There are currently a paucity of clinically available antiobesity drugs (7). Most, if not all, of the pharmacologic agents that reduce body weight are designed to induce satiety (7). Some of the common adverse effects associated with the available antiobesity drugs are hypertension and valve disease (8). Although antiobesity drugs elicit approximately 5% weight reduction, people will not be able

ABBREVIATIONS: BAT, brown adipose tissue; β-LGND2, estrogen receptor β–selective ligand; β3AR, β3 adrenergic receptor; CLAMS, Comprehensive Laboratory Monitoring System; ECAR, extracellular acidification rate; ER, estrogen receptor; FBS, fetal bovine serum; FCCP, carbonyl cyanide-4-(trifluoromethoxy)phenylhydrazone; GFP, green fluorescent protein; HFD, high-fat diet; KO, knockout; MSC, mesenchymal stem cell; ND, normal-diet rodent chow; OCR, oxygen consumption rate; oxphos, oxidative phosphorylation; PCA, principal component analysis; PPAR, peroxisome proliferator-activated receptor; TCA, tricarboxylic acid; WAT, white adipose tissue; WT, wild-type

[1] Current affiliation: College of Pharmacy, University of Michigan, Ann Arbor, MI, USA.

[2] Current affiliation: Department of Nutritional Sciences, University of Michigan School of Public Health, Ann Arbor, MI, USA.

[3] Correspondence: Department of Medicine, University of Tennessee Health Science Center, 19 South Manassas, Room 120, Memphis, TN 38103, USA. E-mail: rnaraya4@uthsc.edu

doi: 10.1096/fj.201600787RR

This article includes supplemental data. Please visit *http://www.fasebj.org* to obtain this information.

0892-6638/17/0031-0266 © FASEB

to maintain the weight reduction for prolonged periods, highlighting the need for efficacious and safe alternatives (9). Strategies proposed to be useful in treating obesity, in addition to inducing satiety (10, 11), include enhancing energy expenditure by converting white adipose tissue (WAT) to brown adipose tissue (BAT) or beige adipose tissue (12–14); or increasing metabolism by enhancing the basal metabolic rate, increasing the intensity of physical activity, or using exercise mimetics, if available (15). Although exercise is an option to increase energy expenditure, it is feasible only in ambulatory individuals and not in disabled, morbidly obese individuals with comorbidities. Pharmaceuticals that increase energy expenditure have been considered to be the Holy Grail in achieving the benefits of physical activity in morbidly obese individuals (15). Although such exercise mimetics have not yet been approved by the U.S. Food and Drug Administration for clinical use, previous studies with the AMPK activators metformin and 5-aminoimidazole-4-carboxamide ribonucleotide (AICAR) have suggested that such therapeutic goals are achievable (16).

Although the beneficial effects of estrogens on adipose and cholesterol metabolism as well as on the cardiovascular system have been demonstrated, data on the receptor or receptors that mediate these positive effects have been conflicting (17–19). The sexually dimorphic anatomy of BAT in females supports the hypothesis that estrogens might be responsible for synthesizing BAT or for converting WAT to BAT (20). The difference in body composition between pre- and postmenopausal women clearly indicates the beneficial effect of estrogens in adipose biology. Studies have shown that administration of estradiol to ovariectomized rats or mice reduces obesity (21), supporting the hypothesis that estrogens are responsible for tightly regulating body weight in women. In addition to favorable effects on adipose tissue, estrogens also attenuate hyperphagia through ER-α (22, 23) and through actions in the central nervous system (24, 25), all culminating in weight loss.

The pharmacologic functions of estrogens are mediated principally by estrogen receptors (ERs) α and β as well as by a membrane receptor (26–28). *In vitro* and *in vivo* models provide evidence for the involvement of these receptors in obesity and cholesterol metabolism (29–31). Support for the antiobesity effects of ER-β ligands is buttressed by studies examining phytoestrogens such as flavonoids and isoflavones (32). The synthetic ER-β agonists estrogen receptor β–selective ligand (β-LGNDs; GTx, Inc., Memphis, TN, USA) and 8β-VE2 have been shown to have antiobesity and antimetabolic diseases effects (31, 33). An advantage of using ER-β-selective ligands as opposed to estradiol to promote weight loss is the lack of cross-reactivity with ER-α. Although these findings support the concept that ER-β-selective ligands have antiobesity and antimetabolic diseases properties, the mechanism by which these molecules elicit the effect is unclear.

Although ER-α has stronger physiologic role in females than in males, the role of ER-β does not appear to depend on sex. Despite the robust functional role of ER-α in females, ER-α knockout (KO) male mice, but not female mice, demonstrated an 11% reduction in energy expenditure with concomitant 20% increase in epididymal and perirenal adipocytes (34). Another study demonstrated a more pronounced effect of ER-α KO in male mice, with 100% increase in adipose size compared to wild-type (WT) male mice (35). This evidence suggests that ER-α and ER-β have significant functional relevance in tissues such as adipose and brain (36, 37) in both males and females despite the widespread perception that they are functionally pertinent only to females.

We found that β-LGND2, also known as GTx-878 (GTx, Inc. (31)), reduces body weight and fat mass without altering feed consumption of high-fat diet (HFD)-fed WT, but not ER-βKO, mice. *In vitro* and *in vivo* studies suggest that β-LGND2 significantly reduces the expression of genes associated with WAT along with increasing the expression of genes associated with BAT. β-LGND2 increases oxygen consumption and mitochondrial activity without increasing physical activity at both 25 and 18°C, a phenomenon predominantly associated with exercise mimetics. These results collectively support our conclusion that ER-β-selective ligands might confer antiobesity effects by altering adipose metabolism and by increasing energy expenditure. They thus may serve as potential targets for clinical development.

MATERIALS AND METHODS

The sources of the reagents used are provided in Supplemental Table 3. All *in vivo* experiments were performed in mice aged 6 to 8 wk at the initiation of the experiment. C57BL6/J mice were used for experiments conducted with WT, while ER-βKO (004745) and ob/ob (000632) mice obtained from The Jackson Laboratory (Bar Harbor, ME, USA) were used for experiments with transgenic mice. All animals were maintained in 12 h dark/light cycle with room temperature maintained at 21°C. Animals had access to food and water *ad libitum*. All animal experiments were carried out in accordance with a University of Tennessee Health Science Center animal care and use committee–approved protocol.

High-fat diet

HFD studies with WT or ER-βKO mice were performed as described elsewhere (31). Ob/ob mice were maintained on rodent chow (normal diet, ND), and studies were conducted as indicated in the figure captions. β-LGND2 was dissolved in DMSO: PEG-300 (15:85%), and the DMSO:PEG-300 formulation was used as the vehicle. All ND mice were also treated with vehicle. Body weight, food consumption, and body composition using MRI were recorded at regular intervals.

RNA isolation, RNA-Seq, and real-time PCR

RNA was isolated using the Qiagen (Germantown, MD, USA) RNA isolation kit and were further processed for RNA-Seq (Supplemental Methods). Real-time PCR was performed with TaqMan primers and probe on an ABI-7900 real-time PCR machine (Thermo Fisher Scientific, Waltham, MA, USA).

Preadipocyte and mesenchymal stem cell differentiation toward adipocytes

Preadipocyte 3T3-L1 cells and mesenchymal stem cells (MSCs) were differentiated as described earlier (38). Briefly, cells were

plated in 24-well plates at 50,000 cells per well in DMEM + 10% fetal bovine serum (FBS). After 2 to 3 d, when they attained confluence, differentiation medium I containing DMEM + 10% FBS, insulin (1 μg/ml), dexamethasone (250 nM), and IBMX (3-isobutyl-1-methylxanthine) was added to the cells and incubated for 3 to 4 d. After 3 to 4 d, differentiation medium II containing DMEM + 10% FBS and insulin was added and incubated for 2 to 3 d (for a total of 6 d). Cells were imaged during every medium change. After 6 d, medium was replaced with DMEM + 10% FBS and maintained in this medium for 3 d. The same protocol was followed with MSCs, but the medium included rosiglitazone (0.5 μM) to activate peroxisome proliferator-activated receptor (PPAR)-γ. 3T3-L1 cells were stably transfected with lentivirus-expressing green fluorescent protein (GFP), ER-α, or ER-β.

Transactivation

Transactivation studies were performed as previously described (31).

Insulin tolerance test

Mice ($n = 16$) were unfed for 6 h before administration of 0.75 mU/kg insulin (Humulin R; Eli Lilly, Indianapolis, IN, USA) in PBS *via* i.p. injection. Blood glucose was measured from the tail vein with a glucometer (OneTouch Ultra; Lifescan, Johnson & Johnson, New Brunswick, NJ, USA) before and every 15 min after injection for 2 h. Because of heterogeneity in the insulin tolerance test values between animals, outliers were determined by Grubb's test, and the resulting data were analyzed by 1-way ANOVA.

Adipose tissue mitochondrial DNA analysis

Primers were designed for mitochondrial- and nuclear-encoded gene regions to detect mRNA transcript levels of mitochondrial genes from cDNA, as well as mitochondrial DNA copy number from genomic DNA, obtained from adipose tissue. SYBR Green and the appropriate primers were used for detection and amplification of genomic DNA or cDNA *via* quantitative real-time PCR. The specific PCR protocol included an activation cycle of 95°C for 10 min, followed by 45 amplification cycles of 15 s at 95°C, 15 s at 60°C, and 10 s at 73°C and using ABI 7900 real-time PCR (Thermo Fisher Scientific).

Mitochondrial DNA primer sequences (5′–3′) are as follows: *mt-Nd1*, forward: CGTCCCCATTCTAATCGCCA, reverse: ATGGCGTCTGCAAATGGTTG; and *mt-Cytb*, forward: CTTCATGTCGGACGAGGCTT, reverse CCTCATGGAAGG ACGTAGCC.

Bioanalysis

Mitochondrial function was assessed in live 3T3-L1 cells using the XF Cell Mito Stress Test in the XF-24 Extracellular Flux Analyzer (Seahorse Bioscience, North Billerica, MA, USA). A total of 5000 cells were seeded in XF24 plates and differentiated in the presence of 10 nM estradiol or 1 μM β-LGND2. Medium was aspirated, then rinsed in and replaced with nonbuffered DMEM with 25 mM glucose, 2 mM L-glutamine, and 1 mM sodium pyruvate (Sigma-Aldrich, St. Louis, MO, USA), incubated at 37°c for 15 min, and run in a flux analyzer per the manufacturer's protocol. Briefly, oxygen consumption rate (OCR) and extracellular acidification rate (ECAR) were measured every 9 min for a total of 12 reads (*i.e.*, 3 reads per injection and for basal levels). Basal rates were established, followed by an injection of 1 μM oligomycin to block ATP synthesis, allowing for the calculation of coupling efficiency (*i.e.*, basal-less oligomycin treated). Then 0.5 μM carbonyl cyanide-4-(trifluoromethoxy)phenylhydrazone (FCCP) was injected to uncouple hydrogen transport and ATP production; the protonophore artificially inflates proton conductance, and this maximal respiration is due to electron transport and substrate delivery. The difference in the basal and uncoupled OCR yields the spare respiratory capacity of the cells. Next, 0.5 μM rotenone was added to inhibit complex I, providing complete blocking of mitochondrial respiration and oxidative phosphorylation (oxphos) to allow one to access nonmitochondrial respiration and proton leak (*i.e.*, the OCR after all mitochondria respiration is blocked and the difference between OCR after FCCP addition and rotenone, respectively).

Comprehensive Laboratory Monitoring System

Male C57BL6/J mice 6 to 8 wk old were purchased from The Jackson Laboratory and allowed to acclimatize to our animal facility for 1 wk. Animals were then singly housed in a Comprehensive Laboratory Monitoring System (CLAMS; Columbus Instruments, Columbus, OH, USA) in home cage–style cages with locked running wheels. Animals were initially maintained in a humidity- and temperature-controlled enclosure at 25°C and 50% humidity. The first 6 h of data were discarded while the animals explored their new surroundings. After 3 d of chow feeding, all animals were switched to an HFD diet and randomized into vehicle- or drug-treated groups. Vehicle or drugs were administered subcutaneously daily. Throughout the study, oxygen utilization, carbon dioxide production, and ambulatory movement were determined at approximately 21-min intervals. After 2 wk, animals were switched to 18°C over the course of 90 min and monitored for a further 7 d. To analyze the data, mixed linear models were constructed and adjusted using fat-free mass, light/dark cycle, and duration of treatment as covariates, giving the animal a random intercept. Linear models containing or lacking treatment as a covariate were compared *via* chi-square tests using the lme4 package (v. 1.1-9) in R software (R Foundation for Statistical Computing, Vienna, Austria). Respiratory exchange ratio was evaluated similarly, except fat-free mass was not used as a covariate. Ambulatory movement was analyzed using light/dark cycle and duration of treatment as covariates and fit to a Poisson distribution.

Transcriptomic analysis

Total RNA was extracted from adipose tissue using the Qiagen RNA isolation kit, and its quality was verified using the Agilent 2100 Bioanalyzer (Agilent Technologies, Santa Clara, CA, USA). A total of 1 μg of total RNA was enriched for poly A RNA using the Dynabeads mRNA Direct Micro Purification Kit according to the manufacturer's standard protocol (Thermo Fisher Scientific Life Sciences). The resulting enriched RNA samples were then used to prepare barcoded libraries for sequencing using the Ion Total RNAseq V2 kit and the Ion Xpress 1-48 Barcode kit (Thermo Fisher Scientific). Libraries were amplified for 16 cycles, and the quality of the libraries was confirmed on an Agilent Bioanalyzer using a DNA High Sensitivity chip. The libraries were pooled on the basis of concentrations from the High Sensitivity chip, purified on a Pippin Prep gel (Sage Science, Beverly, MA, USA), quantified by the Agilent Bioanalyzer, and sequenced on an Ion Torrent proton sequencer (Thermo Fisher Scientific). The sequencing run here had a mean read length of 168 bp and consisted of a total of 79.3 million reads for the 2 samples (34.5 million for sample 9 and 44.8 million for sample 10). These were aligned to the mouse mm9 transcriptome using RNA-Spliced Transcripts Alignment to Reference (STAR) 2.5.2 tool (*https://github.com/alexdobin/STAR/archive/2.5.2b.tar.gz*). The read counts were gathered and normalized using the trimmed mean of *M* values method. The fold change was calculated, and Student's *t* test was used to determine significance. The Benjamini and Hochberg method was used to calculate the adjusted

P values. Only genes with a 2-fold change and an adjusted value of $P \leq 0.05$ was considered differentially expressed. These data were deposited in the Gene Expression Omnibus (GSE85498; National Center for Biotechnology Information, Bethesda, MD, USA; *https://www.ncbi.nlm.nih.gov/*).

Metabolomics analyses

Metabolomics analyses were performed by Metabolon (Durham, NC, USA).

Statistical analysis

Data obtained from 2 groups were analyzed by Student's *t* test, while data obtained from more than 2 groups were analyzed by 1-way ANOVA.

RESULTS

ER-βKO mice become obese more quickly

Earlier studies demonstrated that ER-βKO mice gain more body weight than WT mice when maintained on an HFD (39). However, the effect of knocking down ER-β on body fat and weight when fed with ND had not previously been established. To address this question, male C57BL6/J and ER-βKO mice were maintained on either ND or HFD, and their body weight and composition measured by MRI at regular intervals. As anticipated, the mice maintained on the HFD gained significantly more body weight and fat than the mice maintained on ND (Supplemental Fig. 1). Interestingly, while ER-βKO mice gained significantly more body weight than the WT mice when maintained on either ND or HFD, the relative gain in body weight (WT *vs.* ER-βKO) was much higher when the ER-βKO mice were maintained on ND than on the HFD (Supplemental Fig. 1*A*). While the ER-βKO mice gained approximately 3 times more body fat than WT mice when fed with ND, ER-βKO mice exhibited a 2-fold increase in body fat than WT mice maintained on HFD (Supplemental Fig. 1*B*). No change in lean mass was observed between WT and ER-βKO mice under these condition (data not shown). An interesting observation made in this study is that the gain in body weight and fat mass are much higher when mice are maintained on ND than HFD. Similarly, the temporal changes in body weight occurred much earlier when mice were fed with ND than HFD.

Although we hypothesize that the lesser magnitude of change could be due to the masking effect of greater weight and fat gain by HFD, further work needs to be performed to establish the mechanism for this difference. These data collectively suggest that ER-β is an important regulator of body composition and accordingly body weight, and that loss of ER-β function is sufficient to promote weight gain.

ER-β-selective ligand reduced body weight and fat gain to a greater degree than clinically available antiobesity drugs

In a previous study, we demonstrated that ER-β-selective ligands have antiobesity properties (31). However, at the time that those studies were performed, the ER-β-selective ligands were not benchmarked against U.S. Food and Drug Administration–approved antiobesity drugs to determine the relative magnitude of effect. In the current study, β-LGND2 (**Fig. 1*A***), an ER-β-selective ligand, was selected from a library to evaluate the role of ER-β and its ligands on adipose biology. In a transactivation assay, β-LGND2 activated ER-β with an EC50 of approximately 2 nM, while it activated ER-α with an EC50 of approximately 52 nM, indicating a selectivity of approximately 25-fold for ER-β (Supplemental Fig. 2).

C57BL6/J mice fed with either ND or HFD were treated with vehicle or 30 mg/kg/d β-LGND2 subcutaneously. In order to compare the magnitude of the effect of β-LGND2 to those observed with currently approved compounds, lorcaserin and orlistat were included in the experiment. Lorcaserin, a 5HT2c receptor agonist, increases pro-opiomelanocortin, leading to satiety (Supplemental Fig. 3) and reduced body weight (40). In our study, the doses used were selected on the basis of published work (41–43). Weekly body weight and feed consumption were recorded, and body composition was measured every third week by MRI. At euthanasia, epididymal adipose tissue was isolated and weighed. HFD-fed, vehicle-treated mice gained significantly more body weight, fat mass, and epididymal adipose tissue than ND-fed mice (Fig. 1*B*), which were significantly reduced by β-LGND2 without altering food consumption (Supplemental Fig. 3). These results confirm our earlier findings (31). The effect of β-LGND2 was consistently better than the effects observed with lorcaserin or orlistat.

Effect of β-LGND2 on metabolic syndrome

β-LGND2 has also been shown to have other beneficial effects on metabolic diseases such as hypercholesterolemia, hyperleptinemia, and hyperglycemia, potentially resulting from alterations in body weight and composition (31). In the current studies, we tested β-LGND2's effects on insulin resistance in obese mice using the insulin tolerance test. In the data outlined in mice shown in Fig. 1*B*, the mice were administered insulin, and blood glucose levels were measured every 15 min over a period of 2 h. HFD-fed, vehicle-treated mice had higher serum glucose levels than ND-fed mice, and this increase was reversed back to ND levels by β-LGND2 (Supplemental Fig. 4). The trend matches our previously reported glucose tolerance test data (31).

In order to determine the effects of β-LGND2 in a model of metabolic syndrome, ob/ob (leptin mutant) mice were used; these animals are morbidly obese and exhibit metabolic syndrome (44). While vehicle-treated ob/ob mice gained approximately 75% body weight and 100% fat mass within 4 wk of study initiation, β-LGND2-treated ob/ob mice gained only 25 to 30% body weight and about 50% fat mass during the same 4-wk period (Fig. 1C). The body weight and fat of β-LGND2-treated ob/ob mice were

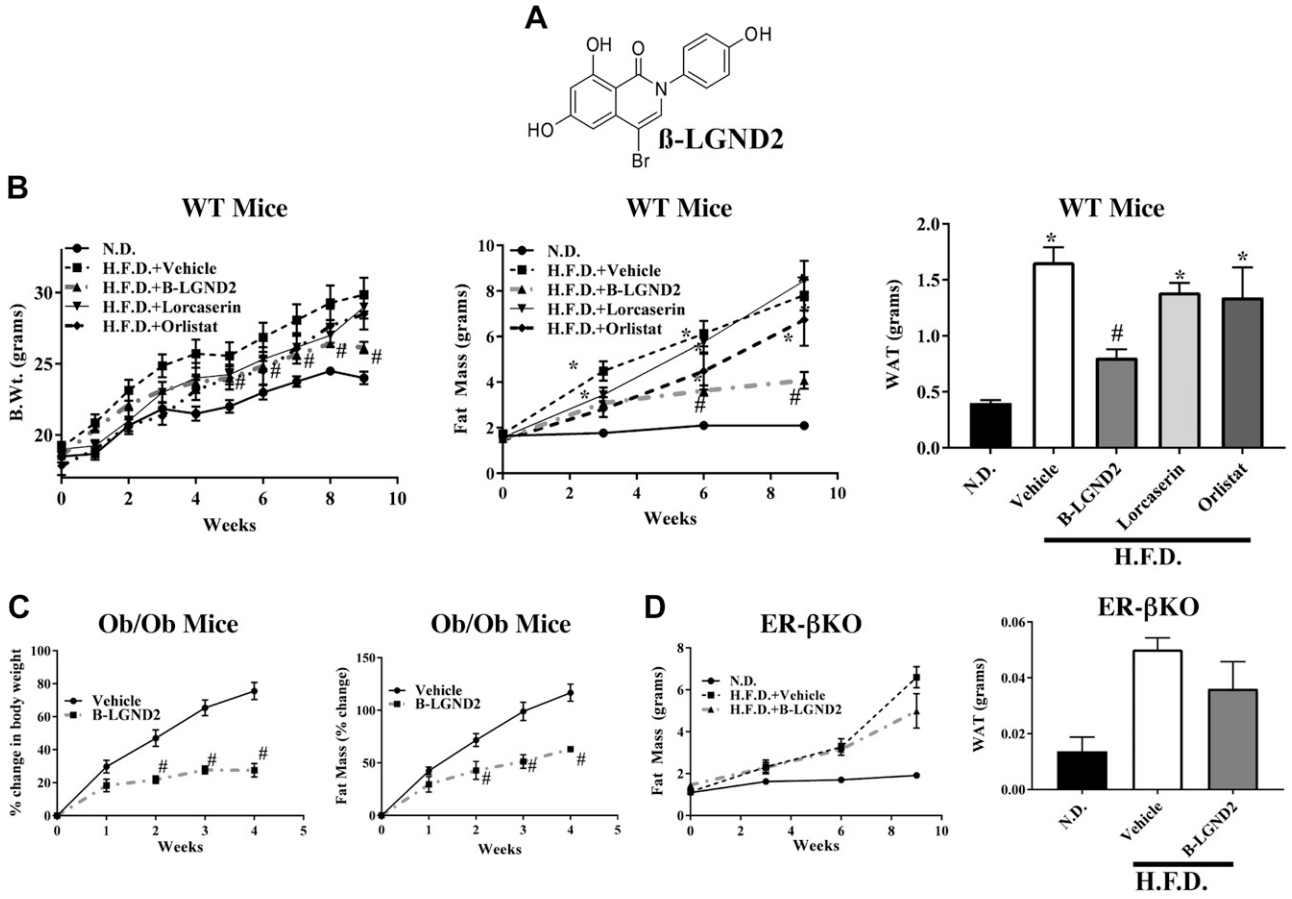

Figure 1. ER-β-selective ligand inhibits obesity. *A*) Structure of β-LGND2. *B*) β-LGND2 inhibits HFD-induced body weight and fat mass better than commercial drugs. Male C57BL6/J mice (6–8 wk old; $n = 6$–7 per group) were fed with ND or HFD. Animals fed with HFD were treated with vehicle, 30 mg/kg/d s.c. β-LGND2, lorcaserin (18 mg/kg/twice daily/s.c.), or orlistat (10 mg/kg/d s.c.). Body weight (left panel) was recorded weekly, and body fat mass (center panel) was measured using MRI once every 3 wk. Animals were humanely killed after 9 wk, and epididymal WAT weight was recorded (right panel). *C*) β-LGND2 inhibits body weight and fat in ob/ob mice. Male ob/ob mice (6–8 wk; $n = 5$) were treated with vehicle or 30 mg/kg/d s.c. β-LGND2. Weekly body weight and fat mass were recorded. Values are represented as percentage change from initiation of experiment. *D*) β-LGND2 inhibits body fat in WT, but not in ER-βKO, male mice. Male WT or ER-βKO mice (6–8 wk old; $n = 6$ per group) were maintained on ND or HFD and treated with vehicle or 30 mg/kg/d s.c. β-LGND2. Body fat was measured once every 3 wk using MRI. Animals were humanely killed, and epididymal WAT weight was recorded. Values are expressed as averages ± SE. Lorc, lorcaserin; Orli, orlistat. $^{*}P < 0.05$ *vs.* ND; $^{\#}P < 0.05$ *vs.* HFD.

significantly lower than vehicle-treated mice. β-LGND2 promoted this effect without affecting feed consumption (Supplemental Fig. 5).

β-LGND2 requires ER-β to function

Earlier studies clearly established that β-LGND2 does not mediate its antiobesity effects through ER-α, as shown by lack of changes in hypothalamus–pituitary–hypogonadal axis, testes weight, or uterus weight in female mice (31). To test whether β-LGND2's effects required ER-β for efficacy, ER-βKO mice were fed an HFD and treated with vehicle or β-LGND2. β-LGND2 failed to prevent body fat gain and epididymal WAT increase in ER-βKO mice (Fig. 1*D*). Although a 20% decrease in WAT mass in β-LGND2-treated ER-βKO mice, compared to 50 to 60% decrease in WT mice, was observed, the change was not statistically significant. These results confirm that β-LGND2 requires ER-β to elicit most of its antiobesity effects.

β-LGND2 inhibited WAT-specific and increased BAT-specific transcripts in epididymal WAT tissue

In an attempt to understand the mechanisms of action for β-LGND2's antiobesity effects, we performed RNA sequencing studies in WAT obtained from animals (Fig. 1*B*). RNA from WAT was isolated and sequenced using an Ion Torrent next-generation sequencer. While the HFD up-regulated the expression of 326 genes ($q < 0.05$ and 2-fold change) and down-regulated the expression of 26 genes compared to the ND, β-LGND2 up-regulated the expression of 153 genes and down-regulated the expression of 126 genes compared to HFD-fed, vehicle-treated mice (**Fig. 2*A***). While feeding

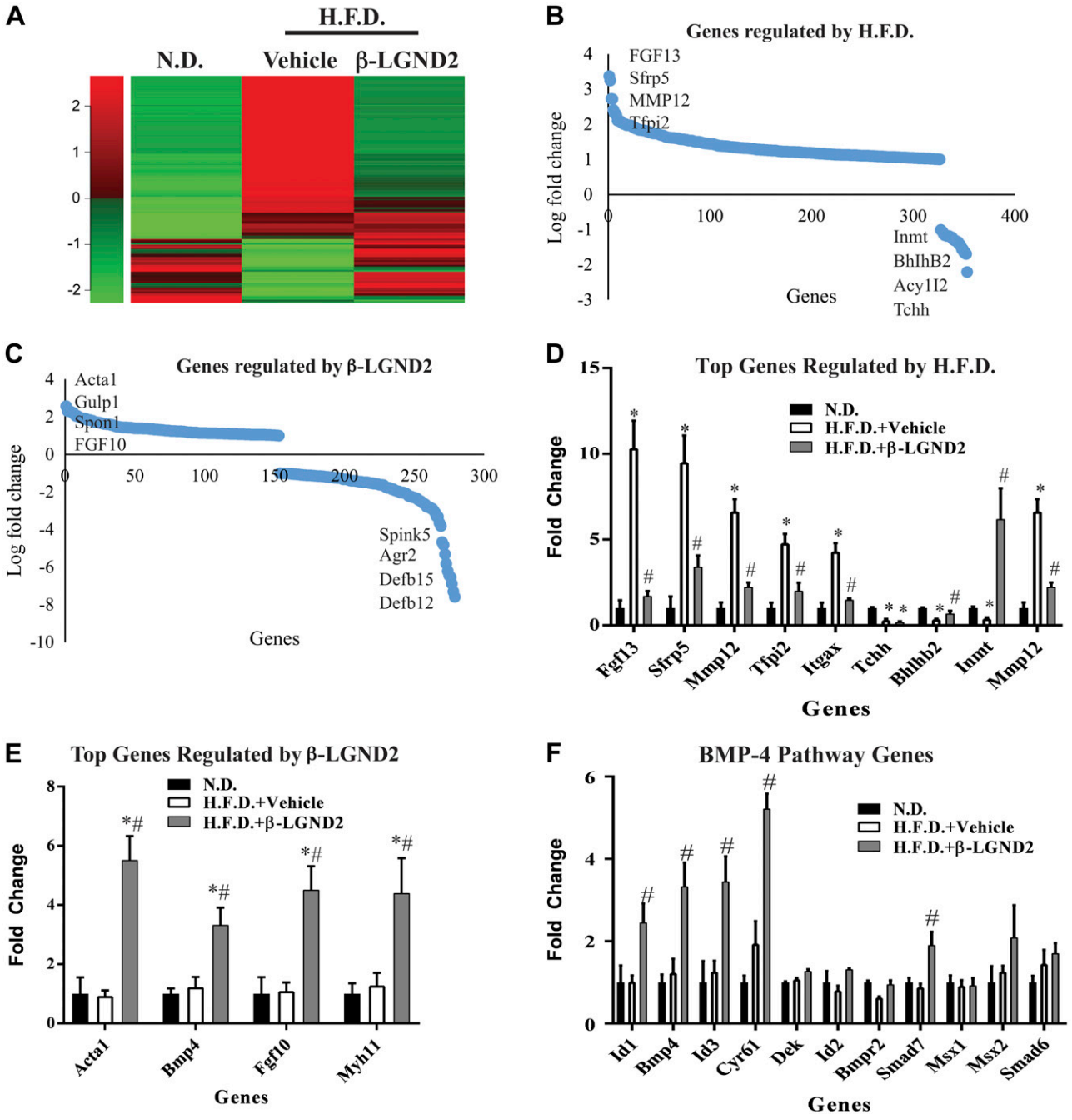

Figure 2. ER-β-selective ligand increases expression of marker genes associated with BAT in WAT. *A*) RNA from epididymal WAT from mice ($n = 3$ per group) shown in Fig. 1*B* was sequenced using Ion Torrent next-generation sequencer. Significantly different genes are expressed in heat map. *B, C*) Genes regulated by HFD (*B*) and β-LGND2 (*C*) are represented as fold change. *D*) Top genes regulated in HFD-fed mice compared to ND-fed mice. *E*) Top genes (based on *P* value) that were up-regulated by β-LGND2 compared to HFD vehicle-treated samples are represented. *F*) Genes representing BMP4 signaling pathway. Values are represented as average ± SE fold change from ND vehicle-treated animals or from HFD vehicle-treated animals. $^{*}P < 0.05$ *vs.* ND; $^{\#}P < 0.05$ *vs.* HFD.

mice with an HFD significantly changed the pattern of the genes compared to ND-fed mice, this pattern was reversed back to the levels observed in ND-fed mice by β-LGND2. The numbers of genes regulated by HFD and β-LGND2 are shown as log fold change in Fig. 2*B*, *C*, respectively, clearly demonstrating that the number of genes up-regulated by HFD was more than the number of genes inhibited by HFD. Alternatively, the magnitude fold of inhibition by β-LGND2 was much higher than the fold activation of the genes by β-LGND2.

A search of the literature provided us with a list of adipogenic, WAT, BAT, or beige adipose tissue marker genes (45, 46). Although it is known that rodents have BAT, only recently has BAT been identified in humans (20, 47). Of the 15 previously described BAT marker genes, in our study, 7 were increased by β-LGND2 (RNA

sequencing data). BAT marker genes that were up-regulated by β-LGND2 include *Ebf2, Foxc2, Pdk4,* and *Tbx2.* These genes have been shown to be critical for the formation of brown adipocytes, mitochondrial function, and mitochondriogenesis (48–50). These results point toward BAT-like characteristics of WAT.

BAT marker genes that were shown to be down-regulated during the formation of BAT were also analyzed in this data set. While all of the genes that inhibit BAT function were up-regulated in WAT of vehicle-treated HFD-fed mice, 5 of 6 of the genes belonging to this class were down-regulated by β-LGND2. Genes that were down-regulated by β-LGND2 administration include *CIDEA,* myostatin (*Mstn*), *Sfrp5,* and *Vegf.* Although because of variability between replicates statistical significance was not achieved in some of the up- and down-regulated genes, the trends point toward a reduction in the expression of these genes by β-LGND2. Collectively, these data support the hypothesis that β-LGND2 treatment correlates with BAT-like characteristics in WAT, which subsequently increases energy expenditure and thermogenesis, culminating in body weight reduction.

Genes that are known to be important regulators of adipogenesis and obesity were also identified within the data set (Fig. 2*D*). While HFD altered the expression of these genes, supporting an increase in adiposity, β-LGND2 reversed their expression toward the levels observed in the WAT of mice fed with ND.

The top 10 most up- and down-regulated genes in WAT obtained from β-LGND2-treated animals support the increase in mitochondrial function and energy expenditure (Fig. 2*C, E*). Top up-regulated genes such as *P2rx1, Acta1, Inmt1,* and *Grem2* are important for energy expenditure and oxphos (51–53). Increase in the expression of these genes will result in enhanced mitochondrial function and ATP generation (54, 55). Similarly, all of the top down-regulated genes—*Gpx5, Gm4846, Lcn8-10,* and *Cst11*—inhibit oxphos and energy expenditure (56–58).

Ingenuity pathway analysis suggested that genes belonging to the BMP4 pathway are enriched in samples that were treated with β-LGND2 (Fig. 2*F*). One of the primary functions of BMP4 signaling in WAT is to increase the brown/beige adipose tissue, resulting in enhanced oxphos, mitochondriogenesis, and energy expenditure (59). Several genes, including *BMP4,* are markedly up-regulated in WAT of animals treated with β-LGND2.

Collectively, the gene expression data demonstrate that WAT is reprogrammed toward BAT by β-LGND2, resulting in an increase in oxphos, thermogenesis, and energy expenditure and subsequently a significant decrease in obesity and adipogenesis.

Metabolomics in WAT indicate that treatment with β-LGND2 increased energy expenditure, oxphos, and energy biogenesis by tricarboxylic acid cycle and non-tricarboxylic acid cycle pathways

In order to further probe into the mechanisms of action for the antiobesity effects of β-LGND2, we performed global metabolomics profiling in the WAT isolated from animals for which data are presented in Fig. 1*B*. WAT from mice fed with HFD exhibited an increase in the level of 135 metabolites and a decrease in the level of 49 metabolites compared to the WAT from mice fed with the ND (Supplemental Table 1). On the other hand, treatment with β-LGND2 increased the levels of 123 metabolites and decreased 8 metabolites compared to WAT isolated from HFD-fed, vehicle-treated mice. Similar to the gene expression results, a heat map of the metabolites indicates that their expression was significantly altered by the HFD compared to the ND, which were principally reversed by β-LGND2 (**Fig. 3*A***). Principal component analysis (PCA) of the metabolite levels from individual samples shows that while samples from the ND-fed animals and HFD-fed β-LGND2-treated animals clustered together, especially on component 1, which contained 45% of the metabolites, samples from HFD-fed, vehicle-treated mice clustered distinctly (Fig. 3*B*). Of the 4 samples analyzed, 1 sample in each group was an outlier, indicating the heterogeneity that exists between the animals.

On the basis of the gene expression results demonstrating an increase in markers of BAT in the WAT samples obtained from animals treated with β-LGND2, we queried the metabolome data for metabolites belonging to pathways involved in energy synthesis and expenditure. Two important pathways are critical for energy creation and expenditure. They are the tricarboxylic acid (TCA) cycle and the non-TCA cycle pathways, such as oxphos and glycolysis (60, 61). While levels of 5 of the 6 TCA cycle intermediates were reduced in the WAT samples from vehicle-treated, HFD-fed animals, these intermediates were increased in WAT samples from the β-LGND2-treated, HFD-fed animals (Fig. 3*C*). Both metabolites belonging to the oxphos pathway, acetylphosphate and phosphate, were decreased in vehicle-treated HFD-fed mice and were significantly increased by β-LGND2 treatment (Fig. 3*D*).

Glycolysis is another major non-TCA cycle pathway utilized to create energy (62). Metabolites belonging to glycolysis were significantly inhibited in the WAT samples obtained from HFD-fed, vehicle-treated mice (Fig. 3*E*). β-LGND2 treatment significantly increased these metabolites, further increasing the potential for enhanced ATP synthesis and energy levels.

ER-β, but not ER-α, ligand-dependently inhibited differentiation of preadipocytes and MSCs toward WAT and promoted differentiation toward BAT

RNA sequencing and metabolomics data provide evidence for the formation of BAT by β-LGND2 that results in an increase in energy synthesis and expenditure. These data provide evidence that β-LGND2 either promotes the formation of new BAT from stem cells or converts the existing WAT to BAT (beige adipose tissue). In order to resolve this question, we utilized *in vitro* cell culture experiments where we overexpressed GFP, ER-α, or ER-β in preadipocyte 3T3-L1 cells and in MSCs and differentiated them toward mature adipocytes in the presence or absence of ER-β-selective β-LGND2 or isoform nonselective

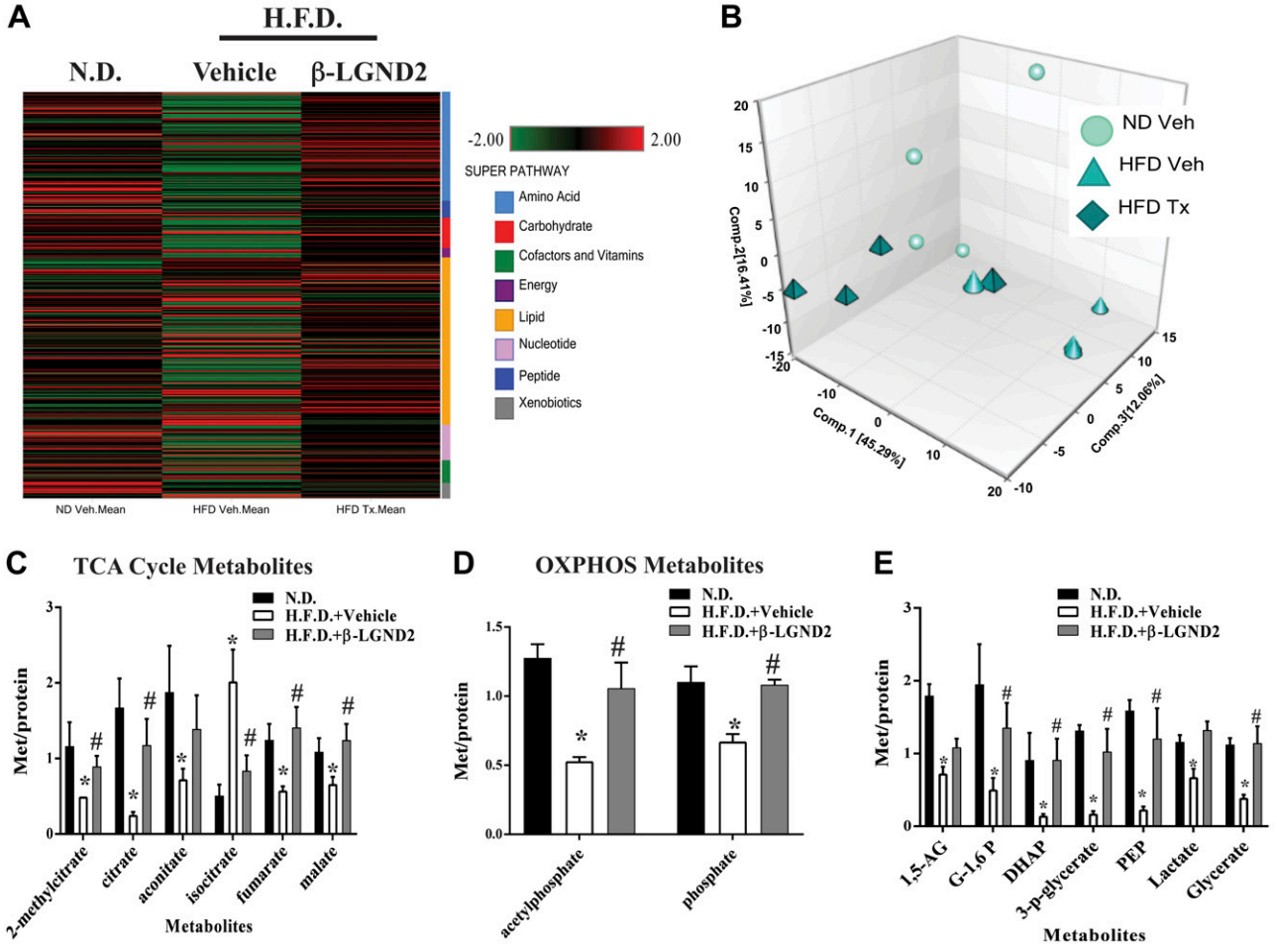

Figure 3. Metabolomics in WAT indicate enhancement of mitochondrial function and energy metabolism by β-LGND2. Metabolites were profiled in WAT obtained from animals ($n = 4$ per group) shown in Fig. 1*B*. *A*) Heat map representing statistically different metabolites. Scale and metabolites category are provided to right of heat map. *B*) PCA shows clustering of individual samples used in metabolite profiling. *C–E*) Significantly different metabolites belonging to TCA cycle (*C*), oxphos (*D*), and glucose metabolism (*E*) are represented. Values are expressed as averages ± SE. $^{*}P < 0.05$ *vs.* ND; $^{\#}P < 0.05$ *vs.* HFD.

estradiol (E2). At the end of 13 d of differentiation, cells were analyzed to determine the type of adipocytes formed (**Fig. 4*A***). While treatment of ER-α-expressing preadipocytes with E2 did not inhibit the formation of oil droplets, treatment of ER-β-expressing preadipocytes with estradiol significantly inhibited the number of oil droplets formed in 3T3-L1 cells (Fig. 4*B*). These results were reproduced when the cells were treated with β-LGND2 (Supplemental Fig. 6).

Expression of WAT- and BAT-related genes was measured in GFP-, ER-α-, and ER-β-expressing 3T3-L1 cells. While ER-α-expressing E2-treated mature adipocytes expressed significantly higher levels of WAT marker genes such as *FABP4* (63, 64), *CEBP-α* (65), and *LIPE* (64), ER-β-expressing, E2-treated mature adipocytes expressed WAT marker genes at lower levels than GFP-transfected cells (Fig. 4*C*, left panel). Contrary to the expression of WAT-related genes, expression of BAT-related genes such as *UCP-1* (66), *ELOVL3* (67), and *CYC1* (68) were all significantly up-regulated in ER-β-expressing E2-treated cells, but not in ER-α-expressing E2-treated cells (Fig. 4*C*, center panel). These results were reproduced with β-LGND2 (Supplemental Fig. 7). Expression of ER-α and ER-β within the cells is shown in Fig. 4*C* (right panel).

Preadipocytes evolve from MSCs (69), which will then differentiate toward WAT or BAT, depending on the environmental stimuli. We stably transfected GFP or ER-β into human MSCs and differentiated them toward mature adipocytes in the presence of β-LGND2 or E2 (Fig. 4*A*). Treatment of ER-β-expressing MSCs with β-LGND2 significantly inhibited the expression of WAT marker genes such as *LPL* and *CEBPα* and concurrently increased the expression of BAT marker genes such as *UCP-1* and *CYC-1* (Fig. 4*D*). These results confirm the data obtained in preadipocyte 3T3-L1 and also provide evidence that ER-β and its ligands differentiate stem cells toward BAT and away from WAT.

In order to determine whether ER-β and its ligands will switch preadipocytes that have already embarked on a differentiated path, we differentiated 3T3-L1 cells as described in Fig. 4*A*, but we initiated treatment on various days during differentiation (Fig. 4*E*) and measured the expression of the BAT marker gene *UCP-1*. While

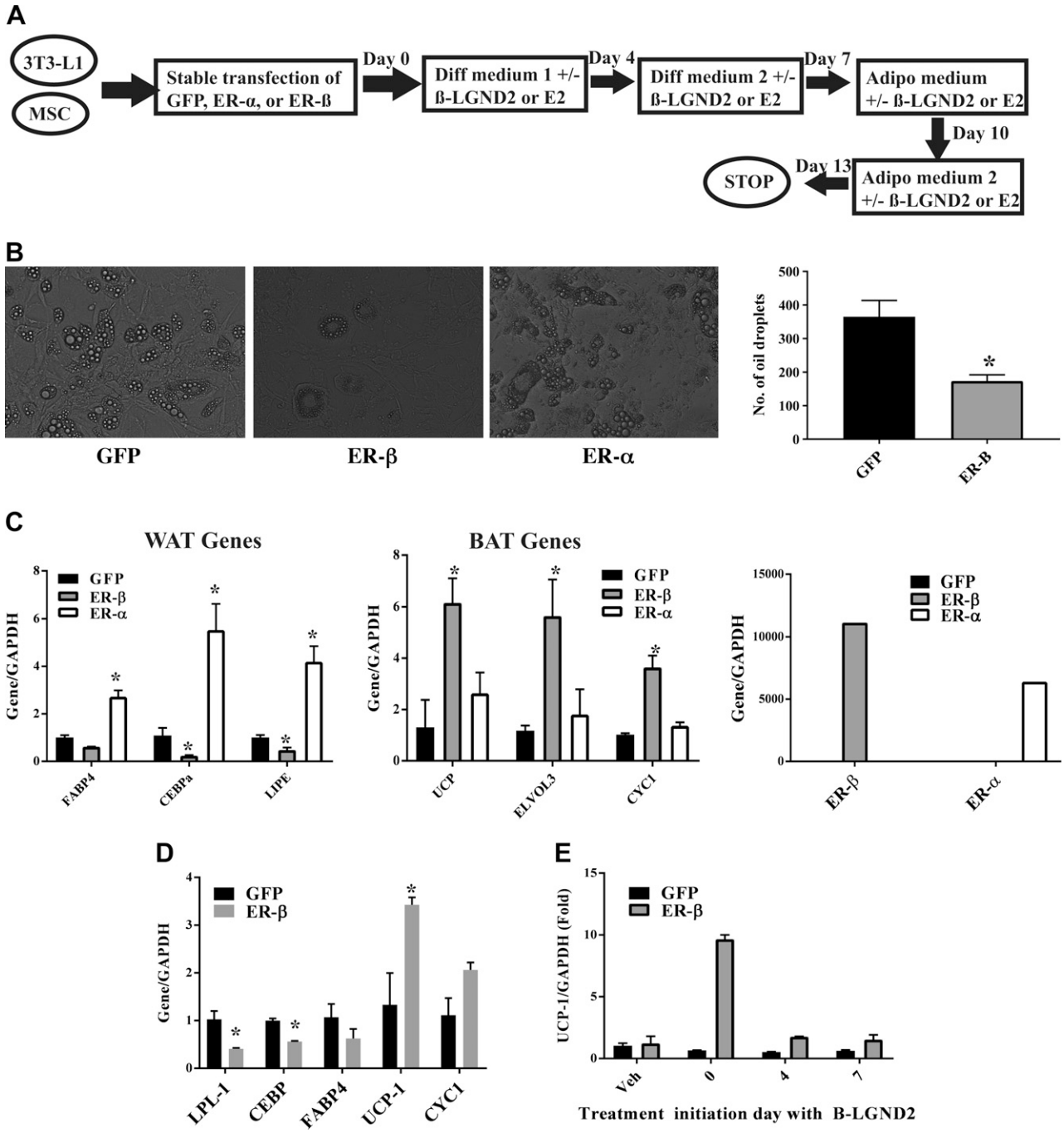

Figure 4. ER-β inhibits preadipocyte and MSC differentiation toward adipocytes and increases BAT marker genes. *A*) Schematic showing experimental design adopted to differentiate preadipocytes 3T3-L1 and MSCs toward mature adipocytes. *B*) Overexpression of ER-β inhibits differentiation of preadipocytes. 3T3-L1 cells stably transfected with GFP, ER-α, or ER-β lentivirus were differentiated in presence of 10 nM estradiol as indicated in *A*. At the end of 14 d, oil droplets were imaged under a microscope. Representative image is shown. Numbers of oil droplets in 10 random fields from each transfection were quantified and are represented in right panel. *C*) Expression of ER-β ligand-dependently increases expression of BAT marker genes. 3T3-L1 cells were stably transfected with GFP, ER-β, or ER-α. Cells were differentiated toward mature adipocytes in presence of 10 nM estradiol for 14 d, as depicted in *A*. At the end of 14 d, RNA was isolated, and expression of WAT (left panel) and BAT (right panel) marker genes was quantified using real-time PCR and normalized to expression of glyceraldehyde phosphate dehydrogenase (GAPDH), and expression of ER-α and ER-β was quantified (right panel). *D*) ER-β inhibits differentiation of MSCs toward mature adipocytes. MSCs stably transfected with GFP or ER-β were differentiated as described in presence of 1 μM β-LGND2. At the end of 14 d, RNA was isolated, and expression of WAT (*LPL-1, CEBP,* and *FABP4*) and BAT (*UCP-1* and *CYC1*) marker genes was quantified using real-time PCR and normalized to expression of GAPDH. *E*) Time course of *UCP-1* induction by β-LGND2 in ER-β-expressing adipocytes. GFP- or ER-β-expressing 3T3-L1 cells were differentiated toward mature adipocytes and treated (1 μM β-LGND2) on different days of differentiation. *UCP-1* expression was quantified and normalized to expression of GAPDH. Values are expressed as averages ± SE. $^{*}P < 0.05$ *vs.* ND; $^{\#}P < 0.05$ *vs.* HFD.

treatment initiation of ER-β-expressing cells with β-LGND2 on day 0 significantly increased the expression of *UCP-1*, treatment initiation on days 4 or 7 failed to induce the *UCP-1* expression (Fig. 4*E*).

β-LGND2 treatment increased oxygen consumption without increasing physical activity of mice

All of the above described studies point toward an increase in the formation of BAT by ER-β and its ligands. If this hypothesis is true, formation of more BAT will increase oxygen consumption and body temperature as a result of an increase in thermogenesis. To test this, C57BL6/J mice were fed a HFD and treated with vehicle or β-LGND2. The mice were maintained at 25°C in CLAMS to continuously monitor oxygen consumption, respiratory exchange ratio, and activity. β-LGND2 treatment and HFD exposure were initiated 48 h after acclimatization of the animals to the CLAMS. Vehicle-treated and β-LGND2-treated animals had similar oxygen consumption and activity scores for the first 48 h of acclimatization (**Fig. 5*A***). Oxygen consumption in the animals treated with β-LGND2 remarkably increased over the next 6 d by 21% ($P = 1.8e\text{-}131$) (Fig. 5*A*, left panel). This increase in oxygen consumption was not a result of ambulatory activity (Fig. 5*A*, right panel), indicating that these mice are burning more energy and generating body heat without changing their physical activity. This magnitude of oxygen consumption increase widened over next 6 d. There was no change in respiratory exchange ratio, body weight, or fat mass in the β-LGND2-treated animals (Supplemental Fig. 8), indicating that the increase in metabolic rate and energy expenditure precedes the previously observed antiobesity effects (Fig. 1*B*).

One of the properties of BAT is to increase core body temperature, resulting in cold tolerance. In order to evaluate the performance of β-LGND2-treated animals under cold exposure, CLAMS temperature was decreased to 18°C after 15 d at 25°C, and oxygen consumption and activity score were measured while animals continued to receive treatment (Fig. 5*B*). As expected, cold exposure immediately and significantly increased oxygen consumption in both groups, with β-LGND2-treated mice immediately exhibiting a further 12.4% increase. The β-LGND2-treated mice continued to maintain the significant difference in oxygen consumption compared to the vehicle-treated mice.

Increase in core body temperature is another confirmation of increased energy expenditure. Core body temperature was measured in mice fed an HFD and treated with vehicle or β-LGND2 (Fig. 5C). β-LGND2-treated mice had a higher body core temperature than vehicle-treated mice.

β-LGND2 treatment increased mitochondrial gene expression in WAT

One of the hallmarks of energy expenditure is an increase in mitochondrial activity (60). To determine whether β-LGND2 increased mitochondrial gene expression as a measure of mitochondriogenesis and mitochondrial function, RNA was isolated from WAT of mice maintained at 25°C or at 18°C and fed with HFD and treated with vehicle or β-LGND2. Expression of mitochondrial and nuclear genes was measured by real-time PCR. As expected, cold exposure increased mitochondrial gene cytochrome B (*CytB*) significantly (Fig. 5*D*, left panel). WAT from HFD-fed, β-LGND2-treated mice exhibited significantly higher expression of *CytB* by over 100-fold compared to that obtained from HFD-fed, vehicle-treated mice (Fig. 5*D*, center panel). Similar to samples from mice exposed to 25°C, WAT from mice treated with β-LGND2 and exposed to 18°C exhibited significantly higher expression of the mitochondrial genes, *CytB* and *ND1* (Fig. 5*D*, right panel). β-LGND2 also increased *UCP-1* by over 1000-fold and *PGC-1* by 2.5-fold in WAT samples from cold-exposed mice, both of which are markers of BAT (Supplemental Fig. 9).

β-LGND2 and E2 receptor-dependently increased mitochondrial respiration and OCR in preadipocytes

In order to determine whether the increase in oxygen consumption and mitochondrial activity are ER-β dependent, we measured the OCR and ECAR in cells using the Seahorse Bioanalyzer. Preadipocytes that were stably transfected with GFP or ER-β were plated and differentiated as described in Fig. 4*A* in the presence or absence of E2 or β-LGND2. Ten days after differentiation, live cells were analyzed in the Seahorse Bioanalyzer. OCR and ECAR were significantly different in E2 and β-LGND2-treated ER-β-expressing cells compared to E2- and β-LGND2-treated GFP-expressing cells (Fig. 5*E*). These results support our *in vivo* findings in the WAT samples and in animals in the CLAMS that ER-β and its ligands appear to increase mitochondrial activity.

Identification of serum biomarkers for obesity and β-LGND2 treatment over time

Although favorable changes to body composition and WAT were elicited by β-LGND2 treatment, identification of serum biomarkers for obesity and ER-β-selective ligand would advance the development of drugs and further understand metabolites secreted in serum during these changes. We also isolated serum from experimental animals before initiation of the experiments described in Fig. 1*B* to obtain information on age-related serum biomarkers and the impact of obesity on these markers (Supplemental Table 2). Because the experiment was conducted for a period of 10 wk, any changes in serum metabolites over 10 wk of aging in lean, obese, and treated obese mice will provide information on biomarkers that will be relevant in the aging of normal and obese individuals.

PCA of serum metabolites shows that over time, the metabolite profile of the mice is significantly altered irrespective of diet treatment (**Fig. 6*A***). While the baseline samples cluster distinctly, the other 3 groups (ND, HFD vehicle, and β-LGND-2) clustered. Analysis of the raw

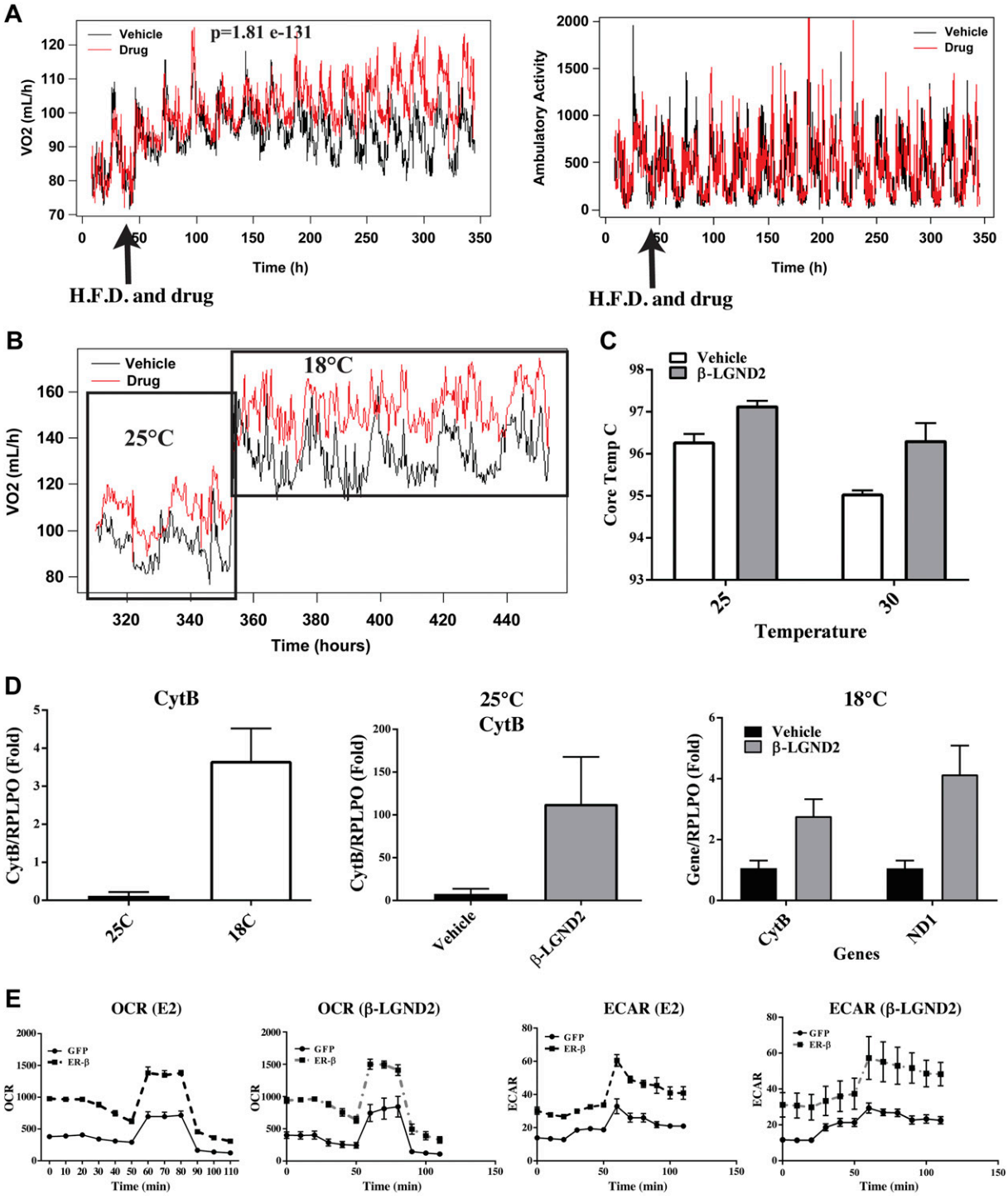

Figure 5. ER-β and its ligands increase oxygen consumption and mitochondrial respiration without increasing physical activity. *A*) Male C57BL6/J mice (6–8 wk old; $n = 8$ per group) fed with HFD and treated with vehicle or 30 mg/kg/d s.c. β-LGND2 were maintained in CLAMS at 25°C for entire duration of experiment. Volume of oxygen (left panel) and ambulatory activity (right panel) were measured constantly 24 h/d. HFD and drug treatment initiation time are indicated by arrow. *B*) Mice ($n = 3$ per group) described in *A* that were maintained at 25°C for first 15 d were exposed to cold (18°C) and continued to receive HFD and vehicle or β-LGND2 treatment. Volume of oxygen consumed was measured constantly 24 h/d. Cold exposure initiation is shown by arrow. *C*) Body core temperature of mice fed with HFD and treated with vehicle or β-LGND2 at 25°C and 30°C. *D*) Mitochondrial marker genes were up-regulated in WAT in animals maintained in cold and in animals treated with β-LGND2. RNA was isolated from WAT of animals shown in *A* and *B*. Expression of mitochondrial genes was measured using real-time PCR and normalized to large ribosomal protein (RPLPO). *E*) OCR and ECAR were increased by ER-β and its ligands. 3T3-L1 cells that were stably transfected with GFP or ER-β were seeded in Seahorse plates and were differentiated in presence or absence of 10 nM estradiol or 1 μM β-LGND2. Ten days after differentiation, mitochondrial respiration was measured with Seahorse Bioanalyzer ($n = 4$). All points on *E* in ER-β transfected cells were significantly different compared to GFP transfected cells. $^{*}P < 0.05$ *vs.* ND; $^{\#}P < 0.05$ *vs.* HFD.

data indicates that most of the metabolites in the serum of ND-fed animals were the nearest representatives of baseline samples. This was followed by the metabolites from the HFD-fed β-LGND2-treated animals.

This concept is represented in the heat map shown in Fig. 6*B*. Although the average of the baseline samples was green across more than 90% of the metabolites, the average of the ND-fed animals showed some increased levels (represented by red), although retaining most of the metabolites at lower levels. Serum metabolites of the β-LGND2-treated, HFD-fed animals could be rank ordered as next to the ND-fed animals, showing more intensity in the expression of the studied metabolites. The HFD-fed, vehicle-treated mice had the highest expression of the serum metabolites. Two categories of metabolites that have the highest expression in the HFD-fed, vehicle-treated are sphingomyelin and fatty acids (Fig. 6*C, D*). While it is expected that the HFD-fed animals would significantly have higher levels of fatty acid metabolites, it is interesting to observe an extremely high expression of metabolites representing the sphingomyelin pathway. While the serum metabolites of ND-fed animals look similar to baseline samples, the metabolites of the HFD-fed, vehicle-treated animals were higher than baseline or ND-fed animals. β-LGND2 partially reduced the intensity of several of the metabolites belonging to the sphingomyelin pathway (Fig. 6*C*). Most, if not all, metabolites were reduced by approximately half by treatment with β-LGND2, and these metabolites were significantly different in samples from β-LGND2-treated animals compared to HFD vehicle-treated animals.

Another set of metabolites that is significantly increased in the HFD-fed animals is the fatty acid or lipid metabolites. Similar to the sphingomyelin metabolites, the level of fatty acid metabolites was also reduced partially by β-LGND2 compared to HFD-fed, vehicle-treated levels (Fig. 6*D*).

DISCUSSION

The *in vitro* and *in vivo* data we present here are summarized in the model depicted in Fig. 6*E*. ER-β and its selective ligands: reprogram MSCs to differentiate toward BAT, rather than WAT; or increase the BAT phenotype by increasing mitochondriogenesis and mitochondrial function. ER-β-selective ligands bound to ER-β induce the expression of genes that promote BAT-like characteristics and inhibit the expression of genes that block BAT formation (Fig. 2). Energy required for thermogenesis by BAT is provided by an increase in glycolysis, TCA cycle, and OXPHOS, all culminating in potential ATP and energy synthesis (Fig. 3). Increases in respiratory rate (Fig. 5) and body temperature dissipate the energy derived from the enhanced mitochondrial biogenesis and biochemical processes of ATP synthesis.

The mitochondria is a unique organelle with its own genome and potential to replicate independent of cell division (70). It is the powerhouse of cells, and cells depend on mitochondria for their energy needs. Metabolomics data (Fig. 3) provide a clear picture of the pathways involved in energy synthesis induced by β-LGND2. BAT formation increases the energy need, which was obtained by glycolysis and the TCA cycle. While aerobic glycolysis promotes the formation of pyruvate, anaerobic glycolysis leads to the formation of lactate. In our metabolomics data, a 5-fold increase in phosphoenoylpyruvate (Supplemental Table 1), which is an end product of aerobic glycolysis, and less than 2-fold increase in lactate formed by β-LGND2 indicate that aerobic glycolysis was the preferred path of glycolysis by β-LGND2. Interestingly, a 5-fold decrease in phosphoenoylpyruvate formation in HFD-fed, vehicle-treated mice indicates the absence of glycolysis and ATP synthesis in obese mice. The pyruvate formed by glycolysis entered TCA cycle (Supplemental Table 1) to generate additional ATP. Oxphos is the main pathway for ATP synthesis from glycolysis and TCA cycle. Changes in metabolites belonging to glycolysis, TCA, and oxphos- and insulin-dependent glucose disposal all support the role of glycolysis and TCA in ER-β function. One of the unknowns at this point is how much ATP was generated by β-LGND2 by burning one molecule of glucose. Although 32 ATPs can be generated from one glucose molecule by glycolysis, TCA cycle, and oxphos combined, it is difficult to achieve this maximum level. Determining the maximum potential of ER-β ligands in this process will help us to understand the distinction of ER-β ligands.

Another interesting observation is the high level of sphingolipids in the serum of HFD-fed, vehicle-treated mice, but not in ND-fed mice or β-LGND2-treated mice (Fig. 6*C*). Sphingolipids have been attributed to, among others, insulin resistance, inflammation, and carcinogenesis (71–73). Detection of high levels of sphingolipids in the serum of obese animals could indicate the potential for susceptibility to many diseases. Interestingly, these sphingolipids were not differentially expressed in the WAT, indicating that either they were synthesized by WAT and secreted into serum or their tissue of origin was different.

Some of the questions that need to be resolved are as follows: Is ER-β expression in the adipose tissue the driving factor for the antiobesity effects of β-LGND2? Does ER-β homodimerize or heterodimerize with ER-α to elicit these effects? How much ATP is formed? The first 2 questions may be addressed by using an adipose-specific KO of ER-β and ER-α. Also, these results have to be extended to other chemical scaffolds of ER-β-selective ligands. Overall, these studies provide evidence for the unique role for ER-β and its ligands in adipose biology.

While estradiol, a non-isoform-selective agonist, reduces food consumption and subsequently body weight, an ER-β-selective agonist such as β-LGND2 reduces body weight without affecting food consumption. Satiety or hyperphagia occur through cross-reactivity with targets in brain. Since β-LGND2 failed to affect food consumption, we speculate that estradiol affects food intake by selectively activating ER-α in brain, which is widely expressed in brain than ER-β (74). Evidences also suggest that estradiol regulates neuropeptide Y and α-melanocyte–stimulating hormone (75), 2 targets important for controlling food intake and energy homeostasis.

Although the functions of ERs are more pronounced in females, the mechanistic studies we describe here were

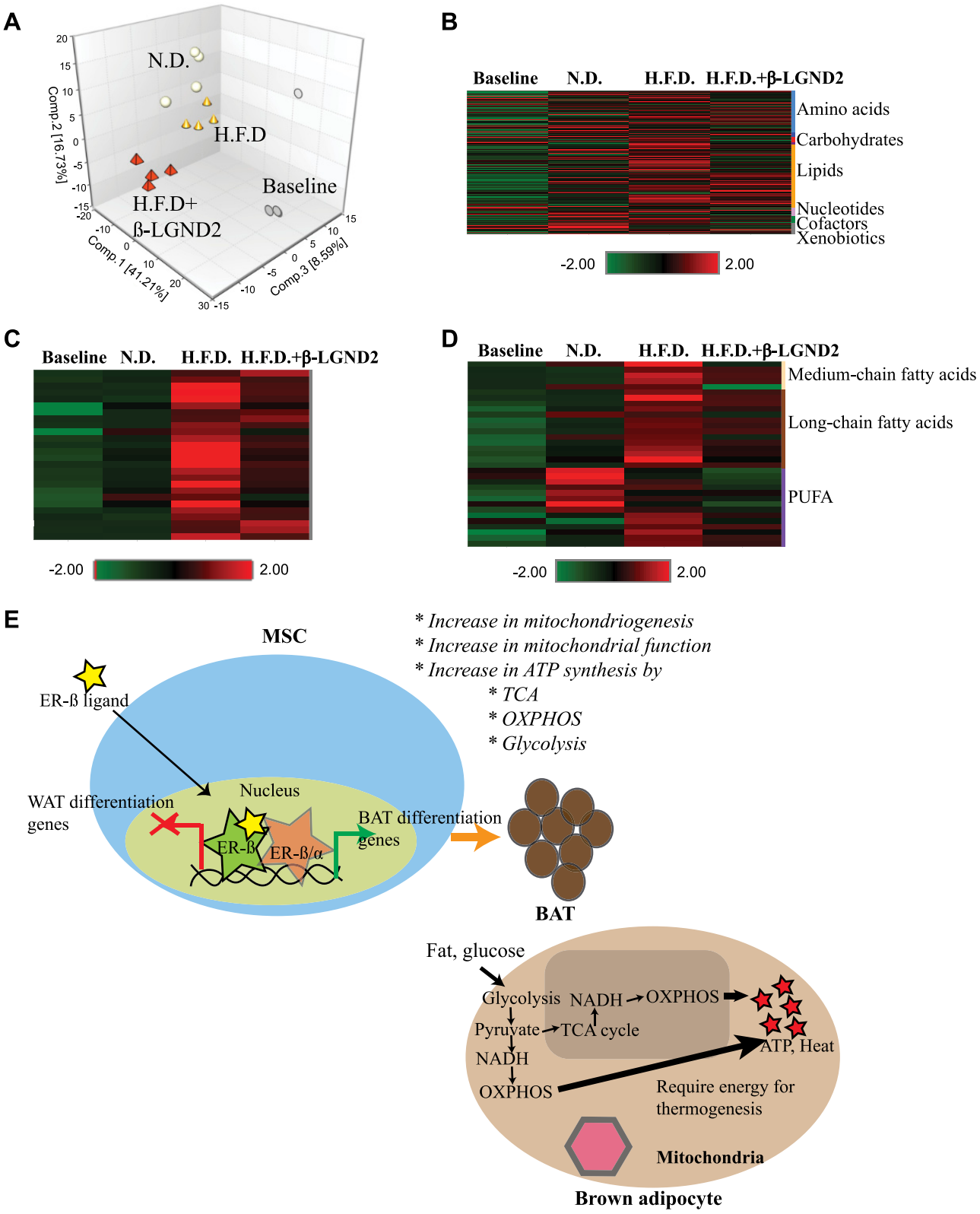

Figure 6. Age-related changes in serum metabolites in lean and obese mice. Metabolites were identified in serum of animals (n = 4 per group) shown in Fig. 1*B*. Serum was isolated from blood at euthanasia, and metabolites were identified. Baseline samples (n = 4) were also obtained before initiation of experiment for comparison with end-of-experiment samples. *A*) PCA shows clustering of individual samples. *B*) Serum metabolites are represented as heat map. *C*, *D*) Pathway-specific metabolites belonging to sphingolipid (*C*) and fatty acid (*D*) metabolism are represented as heat maps. *E*) Model for action of ER-β in adipocytes.

performed in male mice in order to eliminate the interference of circulating estradiol. We earlier demonstrated the efficacy of β-LGNDs in ovariectomy-induced female obesity models (31). Since the studies described in here were conducted to evaluate the mechanism of action of ER-β and its selective ligands, circulating estradiol in female mice that activates both ER-α and ER-β might complicate the outcome and interpretation of the results. To evaluate the effect of ER-β-selective ligand in female mice, mice have to be ovariectomized to reduce circulating estradiol and then supplemented with an HFD in the presence or absence of β-LGNDs. This can introduce another variability of altered hormonal milieu while evaluating the mechanism of action. In addition, previous publications have described sex differences in ER-β expression, with male mouse tissues expressing higher levels than female mouse tissues (36, 37). Future mechanistic studies have to be conducted to explore the mechanism of action in preclinical models of postmenopausal obesity in female mice.

Pharmacologic intervention to increase the BAT has been a subject of significant interest and research. Agonists of PPAR-ɣ, β3 adrenergic receptor (β3AR), and FGF-21, inhibitors of JAK, antagonists of LXR, and agonists of FXR have provided promising results to increase BAT or convert WAT to BAT or beige fat in preclinical models (13, 76–78). ER-β-selective ligands now fall under the class of molecules that have the potential to increase BAT or beige fat. Because of the significant increase in oxygen consumption without a concomitant increase in physical activity, these molecules could also be classified as exercise mimetics. One of the concerns of activating β3AR and PPAR-ɣ is cardiovascular toxicity (76). Earlier studies have shown that β-LGND2 through ER-β reduced cardiac hypertrophy and fibrosis in angiotensin-induced hypertensive models, alleviating concerns of cardiotoxicity due to this pathway (79–81).

Functional BAT has been clearly demonstrated in humans. Five percent of women and 1.3% of men recruited to a study expressed BAT (82). Body weight of BAT-positive individuals was approximately 5 kg lower than individuals lacking BAT (82). *UCP-1*-expressing functional BAT is stimulated by cold exposure. If pharmacologic approaches such as β-LGND2 could achieve this at room temperature, many obese individuals living in tropical regions where cold exposure cannot be achieved may benefit. Approaches such as *UCP-1*-expressing BAT transplant in humans using hydrogels have been proposed to combat obesity (83). Results from feasibility studies in mice are encouraging. All these clearly demonstrate the importance of BAT or beige adipose tissue in combating obesity. If significant increase in *UCP-1*-expressing functional BAT or beige adipose tissue could be achieved by β-LGND2 without any adverse effects on the cardiovascular system, ER-β and its ligands could become an important player in the fight against obesity and metabolic diseases. FJ

ACKNOWLEDGMENTS

The authors thank M. Lee Barret, M. Star, and N. Koehler all from the University of Tennessee Health Science Center) for their help with the animal studies. The authors also thank R. H. Getzenberg (GTx, Inc.) for reviewing an early version of the article. Part of the work was supported by U.S. National Institutes of Health, National Institute of Diabetes and Digestive and Kidney Diseases Grant DK107575, a Memphis Research Consortium grant (to D.B.), and the Quigley Award (to I.H.).

AUTHOR CONTRIBUTIONS

S. Ponnusamy, I. Harvey, H. S. Smallwood, T. Thiyagarajan, S. Banerjee, and R. D. Sullivan performed the experiments; D. Bridges and R. Narayanan designed the experiments; J. T. Dalton and D. D. Miller provided reagents; D. Bridges, Q. T. Tran, and D. L. Johnson analyzed data; R. Narayanan wrote the manuscript; and R. Narayanan is a consultant to GTx, Inc.

REFERENCES

1. Flegal, K. M., Carroll, M. D., Kit, B. K., and Ogden, C. L. (2012) Prevalence of obesity and trends in the distribution of body mass index among U.S. adults, 1999–2010. *JAMA* **307**, 491–497
2. Ogden, C. L., Carroll, M. D., Kit, B. K., and Flegal, K. M. (2014) Prevalence of childhood and adult obesity in the United States, 2011–2012. *JAMA* **311**, 806–814
3. Shrager, B., Jibara, G. A., Tabrizian, P., Roayaie, S., and Ward, S. C. (2012) Resection of nonalcoholic steatohepatitis–associated hepatocellular carcinoma: a Western experience. *Int. J. Surg. Oncol.* **2012**, 915128
4. Jensen, M. D., Ryan, D. H., Apovian, C. M., Ard, J. D., Comuzzie, A. G., Donato, K. A., Hu, F. B., Hubbard, V. S., Jakicic, J. M., Kushner, R. F., Loria, C. M., Millen, B. E., Nonas, C. A., Pi-Sunyer, F. X., Stevens, J., Stevens, V. J., Wadden, T. A., Wolfe, B. M., and Yanovski, S. Z.; American College of Cardiology/American Heart Association Task Force on Practice Guidelines; Obesity Society. (2014) 2013 AHA/ACC/TOS guideline for the management of overweight and obesity in adults: a report of the American College of Cardiology/American Heart Association Task Force on Practice Guidelines and the Obesity Society. *J. Am. Coll. Cardiol.* **63**(25 Pt B), 2985–3023 . Erratum in: *J. Am. Coll. Cardiol.* 2014;63(25 Pt B), 3029–3030
5. Bray, G. A., and Gray, D. S. (1988) Obesity. Part I—pathogenesis. *West. J. Med.* **149**, 429–441
6. Madden, N. (2015) Obesity weighing down U.S. economy, study finds [electronic version]. *Washington Times*. Retrieved September 19, 2016, from http://www.washingtontimes.com/news/2015/may/13/obesity-weighing-down-us-economy-study-finds/
7. Jones, B. J., and Bloom, S. R. (2015) The new era of drug therapy for obesity: the evidence and the expectations. *Drugs* **75**, 935–945
8. Cunningham, J. W., and Wiviott, S. D. (2014) Modern obesity pharmacotherapy: weighing cardiovascular risk and benefit. *Clin. Cardiol.* **37**, 693–699
9. Patel, D. (2015) Pharmacotherapy for the management of obesity. *Metabolism* **64**, 1376–1385
10. Smith, S. R., Weissman, N. J., Anderson, C. M., Sanchez, M., Chuang, E., Stubbe, S., Bays, H., Shanahan, W. R., and Behavioral, M.; Behavioral Modification and Lorcaserin for Overweight and Obesity Management (BLOOM) Study Group. (2010) Multicenter, placebo-controlled trial of lorcaserin for weight management. *N. Engl. J. Med.* **363**, 245–256
11. Mercken, E. M., Carboneau, B. A., Krzysik-Walker, S. M., and de Cabo, R. (2012) Of mice and men: the benefits of caloric restriction, exercise, and mimetics. *Ageing Res. Rev.* **11**, 390–398
12. Lee, Y. K., and Cowan, C. A. (2013) White to brite adipocyte transition and back again. *Nat. Cell Biol.* **15**, 568–569
13. Moisan, A., Lee, Y. K., Zhang, J. D., Hudak, C. S., Meyer, C. A., Prummer, M., Zoffmann, S., Truong, H. H., Ebeling, M., Kiialainen, A., Gérard, R., Xia, F., Schinzel, R. T., Amrein, K. E., and Cowan, C. A. (2015) White-to-brown metabolic conversion of human adipocytes by JAK inhibition. *Nat. Cell Biol.* **17**, 57–67
14. Roberts, L. D., Boström, P., O'Sullivan, J. F., Schinzel, R. T., Lewis, G. D., Dejam, A., Lee, Y. K., Palma, M. J., Calhoun, S., Georgiadi, A.,

Chen, M. H., Ramachandran, V. S., Larson, M. G., Bouchard, C., Rankinen, T., Souza, A. L., Clish, C. B., Wang, T. J., Estall, J. L., Soukas, A. A., Cowan, C. A., Spiegelman, B. M., and Gerszten, R. E. (2014) β-Aminoisobutyric acid induces browning of white fat and hepatic β-oxidation and is inversely correlated with cardiometabolic risk factors. *Cell Metab.* **19**, 96–108
15. Fan, W., Atkins, A. R., Yu, R. T., Downes, M., and Evans, R. M. (2013) Road to exercise mimetics: targeting nuclear receptors in skeletal muscle. *J. Mol. Endocrinol.* **51**, T87–T100
16. Narkar, V. A., Downes, M., Yu, R. T., Embler, E., Wang, Y. X., Banayo, E., Mihaylova, M. M., Nelson, M. C., Zou, Y., Juguilon, H., Kang, H., Shaw, R. J., and Evans, R. M. (2008) AMPK and PPARdelta agonists are exercise mimetics. *Cell* **134**, 405–415
17. Bhardwaj, P., Du, B., Zhou, X. K., Sue, E., Giri, D., Harbus, M. D., Falcone, D. J., Hudis, C. A., Subbaramaiah, K., and Dannenberg, A. J. (2015) Estrogen protects against obesity-induced mammary gland inflammation in mice. *Cancer Prev. Res. (Phila.)* **8**, 751–759
18. Luglio, H. F. (2014) Estrogen and body weight regulation in women: the role of estrogen receptor alpha (ER-α) on adipocyte lipolysis. *Acta Med. Indones.* **46**, 333–338
19. Davis, K. E., Carstens, E. J., Irani, B. G., Gent, L. M., Hahner, L. M., and Clegg, D. J. (2014) Sexually dimorphic role of G protein–coupled estrogen receptor (GPER) in modulating energy homeostasis. *Horm. Behav.* **66**, 196–207
20. Cypess, A. M., Lehman, S., Williams, G., Tal, I., Rodman, D., Goldfine, A. B., Kuo, F. C., Palmer, E. L., Tseng, Y. H., Doria, A., Kolodny, G. M., and Kahn, C. R. (2009) Identification and importance of brown adipose tissue in adult humans. *N. Engl. J. Med.* **360**, 1509–1517
21. Wang, Y., Shoemaker, R., Thatcher, S. E., Batifoulier-Yiannikouris, F., English, V. L., and Cassis, L. A. (2015) Administration of 17β-estradiol to ovariectomized obese female mice reverses obesity-hypertension through an ACE2-dependent mechanism. *Am. J. Physiol. Endocrinol. Metab.* **308**, E1066–E1075
22. Salamanca, S., and Uphouse, L. (1992) Estradiol modulation of the hyperphagia induced by the 5-HT1A agonist, 8-OH-DPAT. *Pharmacol. Biochem. Behav.* **43**, 953–955
23. Musatov, S., Chen, W., Pfaff, D. W., Mobbs, C. V., Yang, X. J., Clegg, D. J., Kaplitt, M. G., and Ogawa, S. (2007) Silencing of estrogen receptor alpha in the ventromedial nucleus of hypothalamus leads to metabolic syndrome. *Proc. Natl. Acad. Sci. USA* **104**, 2501–2506
24. Santollo, J., and Eckel, L. A. (2013) Oestradiol decreases melanin-concentrating hormone (MCH) and MCH receptor expression in the hypothalamus of female rats. *J. Neuroendocrinol.* **25**, 570–579
25. Rivera, H. M., Santollo, J., Nikonova, L. V., and Eckel, L. A. (2012) Estradiol increases the anorexia associated with increased 5-HT(2C) receptor activation in ovariectomized rats. *Physiol. Behav.* **105**, 188–194
26. Dierks-Ventling, C., and Bieri-Bonniot, F. (1977) Stimulation of RNA polymerase I and II activities by 17 beta-estradiol receptor on chick liver chromatin. *Nucleic Acids Res.* **4**, 381–395
27. Kuiper, G. G., Enmark, E., Pelto-Huikko, M., Nilsson, S., and Gustafsson, J. A. (1996) Cloning of a novel receptor expressed in rat prostate and ovary. *Proc. Natl. Acad. Sci. USA* **93**, 5925–5930
28. Revankar, C. M., Cimino, D. F., Sklar, L. A., Arterburn, J. B., and Prossnitz, E. R. (2005) A transmembrane intracellular estrogen receptor mediates rapid cell signaling. *Science* **307**, 1625–1630
29. Yoshii, T., Yamada, M., Minami, T., Tsunoda, T., Sasaki, M., Kondo, Y., Satoh, S., and Terauchi, Y. (2015) The effects of bazedoxifene on bone, glucose, and lipid metabolism in postmenopausal women with type 2 diabetes: an exploratory pilot study. *J. Clin. Med. Res.* **7**, 762–769
30. Meyer, M. R., Fredette, N. C., Howard, T. A., Hu, C., Ramesh, C., Daniel, C., Amann, K., Arterburn, J. B., Barton, M., and Prossnitz, E. R. (2014) G protein–coupled estrogen receptor protects from atherosclerosis. *Sci. Rep.* **4**, 7564
31. Yepuru, M., Eswaraka, J., Kearbey, J. D., Barrett, C. M., Raghow, S., Veverka, K. A., Miller, D. D., Dalton, J. T., and Narayanan, R. (2010) Estrogen receptor-beta-selective ligands alle*via*te high-fat diet– and ovariectomy-induced obesity in mice. *J. Biol. Chem.* **285**, 31292–31303
32. Jungbauer, A., and Medjakovic, S. (2014) Phytoestrogens and the metabolic syndrome. *J. Steroid Biochem. Mol. Biol.* **139**, 277–289
33. Weigt, C., Hertrampf, T., Kluxen, F. M., Flenker, U., Hülsemann, F., Fritzemeier, K. H., and Diel, P. (2013) Molecular effects of ER alpha- and beta-selective agonists on regulation of energy homeostasis in obese female Wistar rats. *Mol. Cell. Endocrinol.* **377**, 147–158
34. Heine, P. A., Taylor, J. A., Iwamoto, G. A., Lubahn, D. B., and Cooke, P. S. (2000) Increased adipose tissue in male and female estrogen receptor-alpha knockout mice. *Proc. Natl. Acad. Sci. USA* **97**, 12729–12734
35. Cooke, P. S., Heine, P. A., Taylor, J. A., and Lubahn, D. B. (2001) The role of estrogen and estrogen receptor-alpha in male adipose tissue. *Mol. Cell. Endocrinol.* **178**, 147–154
36. Ivanova, T., and Beyer, C. (2000) Ontogenetic expression and sex differences of aromatase and estrogen receptor-alpha/beta mRNA in the mouse hippocampus. *Cell Tissue Res.* **300**, 231–237
37. Karolczak, M., and Beyer, C. (1998) Developmental sex differences in estrogen receptor-beta mRNA expression in the mouse hypothalamus/preoptic region. *Neuroendocrinology* **68**, 229–234
38. Chiang, S. H., Chang, L., and Saltiel, A. R. (2006) TC10 and insulin-stimulated glucose transport. *Methods Enzymol.* **406**, 701–714
39. Foryst-Ludwig, A., Clemenz, M., Hohmann, S., Hartge, M., Sprang, C., Frost, N., Krikov, M., Bhanot, S., Barros, R., Morani, A., Gustafsson, J. A., Unger, T., and Kintscher, U. (2008) Metabolic actions of estrogen receptor beta (ERbeta) are mediated by a negative cross-talk with PPARgamma. *PLoS Genet.* **4**, e1000108
40. Burke, L. K., Doslikova, B., D'Agostino, G., Garfield, A. S., Farooq, G., Burdakov, D., Low, M. J., Rubinstein, M., Evans, M. L., Billups, B., and Heisler, L. K. (2014) 5-HT obesity medication efficacy *via* POMC activation is maintained during aging. *Endocrinology* **155**, 3732–3738
41. Thomsen, W. J., Grottick, A. J., Menzaghi, F., Reyes-Saldana, H., Espitia, S., Yuskin, D., Whelan, K., Martin, M., Morgan, M., Chen, W., Al-Shamma, H., Smith, B., Chalmers, D., and Behan, D. (2008) Lorcaserin, a novel selective human 5-hydroxytryptamine2C agonist: *in vitro* and *in vivo* pharmacological characterization. *J. Pharmacol. Exp. Ther.* **325**, 577–587
42. Smith, B. M., Smith, J. M., Tsai, J. H., Schultz, J. A., Gilson, C. A., Estrada, S. A., Chen, R. R., Park, D. M., Prieto, E. B., Gallardo, C. S., Sengupta, D., Dosa, P. I., Covel, J. A., Ren, A., Webb, R. R., Beeley, N. R., Martin, M., Morgan, M., Espitia, S., Saldana, H. R., Bjenning, C., Whelan, K. T., Grottick, A. J., Menzaghi, F., and Thomsen, W. J. (2008) Discovery and structure-activity relationship of (1R)-8-chloro-2,3,4,5-tetrahydro-1-methyl-1H-3-benzazepine (lorcaserin), a selective serotonin 5-HT2C receptor agonist for the treatment of obesity. *J. Med. Chem.* **51**, 305–313
43. An, S., Han, J. I., Kim, M. J., Park, J. S., Han, J. M., Baek, N. I., Chung, H. G., Choi, M. S., Lee, K. T., and Jeong, T. S. (2010) Ethanolic extracts of *Brassica campestris* spp. rapa roots prevent high-fat diet–induced obesity *via* beta(3)-adrenergic regulation of white adipocyte lipolytic activity. *J. Med. Food* **13**, 406–414
44. Ingalls, A. M., Dickie, M. M., and Snell, G. D. (1950) Obese, a new mutation in the house mouse. *J. Hered.* **41**, 317–318
45. Wu, J., Boström, P., Sparks, L. M., Ye, L., Choi, J. H., Giang, A. H., Khandekar, M., Virtanen, K. A., Nuutila, P., Schaart, G., Huang, K., Tu, H., van Marken Lichtenbelt, W. D., Hoeks, J., Enerbäck, S., Schrauwen, P., and Spiegelman, B. M. (2012) Beige adipocytes are a distinct type of thermogenic fat cell in mouse and human. *Cell* **150**, 366–376
46. Harms, M., and Seale, P. (2013) Brown and beige fat: development, function and therapeutic potential. *Nat. Med.* **19**, 1252–1263
47. Virtanen, K. A., Lidell, M. E., Orava, J., Heglind, M., Westergren, R., Niemi, T., Taittonen, M., Laine, J., Savisto, N. J., Enerbäck, S., and Nuutila, P. (2009) Functional brown adipose tissue in healthy adults. *N. Engl. J. Med.* **360**, 1518–1525
48. Wang, W., Kissig, M., Rajakumari, S., Huang, L., Lim, H. W., Won, K. J., and Seale, P. (2014) *Ebf2* is a selective marker of brown and beige adipogenic precursor cells. *Proc. Natl. Acad. Sci. USA* **111**, 14466–14471
49. Lidell, M. E., Seifert, E. L., Westergren, R., Heglind, M., Gowing, A., Sukonina, V., Arani, Z., Itkonen, P., Wallin, S., Westberg, F., Fernandez-Rodriguez, J., Laakso, M., Nilsson, T., Peng, X. R., Harper, M. E., and Enerbäck, S. (2011) The adipocyte-expressed forkhead transcription factor Foxc2 regulates metabolism through altered mitochondrial function. *Diabetes* **60**, 427–435
50. Hao, Q., Yadav, R., Basse, A. L., Petersen, S., Sonne, S. B., Rasmussen, S., Zhu, Q., Lu, Z., Wang, J., Audouze, K., Gupta, R., Madsen, L., Kristiansen, K., and Hansen, J. B. (2015) Transcriptome profiling of brown adipose tissue during cold exposure reveals extensive regulation of glucose metabolism. *Am. J. Physiol. Endocrinol. Metab.* **308**, E380–E392
51. Gnad, T., Scheibler, S., von Kügelgen, I., Scheele, C., Kilić, A., Glöde, A., Hoffmann, L. S., Reverte-Salisa, L., Horn, P., Mutlu, S., El-Tayeb, A., Kranz, M., Deuther-Conrad, W., Brust, P., Lidell, M. E., Betz, M. J., Enerbäck, S., Schrader, J., Yegutkin, G. G., Müller, C. E., and Pfeifer, A. (2014) Adenosine activates brown adipose tissue and recruits beige adipocytes *via* A2A receptors. *Nature* **516**, 395–399
52. Liang, J., Xu, Z. X., Ding, Z., Lu, Y., Yu, Q., Werle, K. D., Zhou, G., Park, Y. Y., Peng, G., Gambello, M. J., and Mills, G. B. (2015) Myristoylation confers noncanonical AMPK functions in autophagy selectivity and mitochondrial surveillance. *Nat. Commun.* **6**, 7926

53. Wu, Q., Tang, S. G., and Yuan, Z. M. (2015) Gremlin 2 inhibits adipocyte differentiation through activation of Wnt/β-catenin signaling. *Mol. Med. Rep.* **12**, 5891–5896
54. Li, A., Leung, C. T., Peterson-Yantorno, K., Stamer, W. D., Mitchell, C. H., and Civan, M. M. (2012) Mechanisms of ATP release by human trabecular meshwork cells, the enabling step in purinergic regulation of aqueous humor outflow. *J. Cell. Physiol.* **227**, 172–182
55. Guirguis, E., Hockman, S., Chung, Y. W., Ahmad, F., Gavrilova, O., Raghavachari, N., Yang, Y., Niu, G., Chen, X., Yu, Z. X., Liu, S., Degerman, E., and Manganiello, V. (2013) A role for phosphodiesterase 3B in acquisition of brown fat characteristics by white adipose tissue in male mice. *Endocrinology* **154**, 3152–3167
56. Rupérez, A. I., Olza, J., Gil-Campos, M., Leis, R., Mesa, M. D., Tojo, R., Cañete, R., Gil, Á., and Aguilera, C. M. (2014) Association of genetic polymorphisms for glutathione peroxidase genes with obesity in Spanish children. *J. Nutrigenet. Nutrigenomics* **7**, 130–142
57. Catalán, V., Gómez-Ambrosi, J., Rodríguez, A., Ramírez, B., Silva, C., Rotellar, F., Gil, M. J., Cienfuegos, J. A., Salvador, J., and Frühbeck, G. (2009) Increased adipose tissue expression of lipocalin-2 in obesity is related to inflammation and matrix metalloproteinase-2 and metalloproteinase-9 activities in humans. *J. Mol. Med. (Berl.)* **87**, 803–813
58. Fried, S. K., and Greenberg, A. S. (2012) Lipocalin 2: a "sexy" adipokine that regulates 17β-estradiol and obesity. *Endocrinology* **153**, 1582–1584
59. Gustafson, B., Hammarstedt, A., Hedjazifar, S., Hoffmann, J. M., Svensson, P. A., Grimsby, J., Rondinone, C., and Smith, U. (2015) BMP4 and BMP antagonists regulate human white and beige adipogenesis. *Diabetes* **64**, 1670–1681
60. Heinonen, S., Buzkova, J., Muniandy, M., Kaksonen, R., Ollikainen, M., Ismail, K., Hakkarainen, A., Lundbom, J., Lundbom, N., Vuolteenaho, K., Moilanen, E., Kaprio, J., Rissanen, A., Suomalainen, A., and Pietiläinen, K. H. (2015) Impaired mitochondrial biogenesis in adipose tissue in acquired obesity. *Diabetes* **64**, 3135–3145
61. Schmid, G. M., Converset, V., Walter, N., Sennitt, M. V., Leung, K. Y., Byers, H., Ward, M., Hochstrasser, D. F., Cawthorne, M. A., and Sanchez, J. C. (2004) Effect of high-fat diet on the expression of proteins in muscle, adipose tissues, and liver of C57BL/6 mice. *Proteomics* **4**, 2270–2282
62. Costanzo-Garvey, D. L., Pfluger, P. T., Dougherty, M. K., Stock, J. L., Boehm, M., Chaika, O., Fernandez, M. R., Fisher, K., Kortum, R. L., Hong, E. G., Jun, J. Y., Ko, H. J., Schreiner, A., Volle, D. J., Treece, T., Swift, A. L., Winer, M., Chen, D., Wu, M., Leon, L. R., Shaw, A. S., McNeish, J., Kim, J. K., Morrison, D. K., Tschöp, M. H., and Lewis, R. E. (2009) *KSR2* is an essential regulator of AMP kinase, energy expenditure, and insulin sensitivity. *Cell Metab.* **10**, 366–378
63. Qian, S. W., Tang, Y., Li, X., Liu, Y., Zhang, Y. Y., Huang, H. Y., Xue, R. D., Yu, H. Y., Guo, L., Gao, H. D., Liu, Y., Sun, X., Li, Y. M., Jia, W. P., and Tang, Q. Q. (2013) BMP4-mediated brown fat–like changes in white adipose tissue alter glucose and energy homeostasis. *Proc. Natl. Acad. Sci. USA* **110**, E798–E807
64. Bag, S., Ramaiah, S., and Anbarasu, A. (2015) *fabp4* is central to eight obesity associated genes: a functional gene network–based polymorphic study. *J. Theor. Biol.* **364**, 344–354
65. Rosen, E. D., Hsu, C. H., Wang, X., Sakai, S., Freeman, M. W., Gonzalez, F. J., and Spiegelman, B. M. (2002) C/EBPalpha induces adipogenesis through PPARgamma: a unified pathway. *Genes Dev.* **16**, 22–26
66. Lean, M. E., and James, W. P. (1983) Uncoupling protein in human brown adipose tissue mitochondria. Isolation and detection by specific antiserum. *FEBS Lett.* **163**, 235–240
67. Ji, L., Gupta, M., and Feldman, B. J. (2016) Vitamin D regulates fatty acid composition in subcutaneous adipose tissue through *Elovl3*. *Endocrinology* **1**, 91–97
68. Chrysovergis, K., Wang, X., Kosak, J., Lee, S. H., Kim, J. S., Foley, J. F., Travlos, G., Singh, S., Baek, S. J., and Eling, T. E. (2014) NAG-1/GDF-15 prevents obesity by increasing thermogenesis, lipolysis and oxidative metabolism. *Int. J. Obes.* **38**, 1555–1564
69. Fink, T., and Zachar, V. (2011) Adipogenic differentiation of human mesenchymal stem cells. *Methods Mol. Biol.* **698**, 243–251
70. Chan, D. C. (2006) Mitochondria: dynamic organelles in disease, aging, and development. *Cell* **125**, 1241–1252
71. Choi, S., and Snider, A. J. (2015) Sphingolipids in high fat diet and obesity-related diseases. *Mediators Inflamm.* **2015**, 520618
72. Kurek, K., Mikłosz, A., Łukaszuk, B., Chabowski, A., Górski, J., and Żendzian-Piotrowska, M. (2015) Inhibition of ceramide *de novo* synthesis ameliorates diet induced skeletal muscles insulin resistance. *J. Diabetes Res.* **2015**, 154762
73. Matula, K., Collie-Duguid, E., Murray, G., Parikh, K., Grabsch, H., Tan, P., Lalwani, S., Garau, R., Ong, Y., Bain, G., Smith, A. D., Urquhart, G., Bielawski, J., Finnegan, M., and Petty, R. (2015) Regulation of cellular sphingosine-1-phosphate by sphingosine kinase 1 and sphingosine-1-phopshate lyase determines chemotherapy resistance in gastroesophageal cancer. *BMC Cancer* **15**, 762
74. Pérez, S. E., Chen, E. Y., and Mufson, E. J. (2003) Distribution of estrogen receptor alpha and beta immunoreactive profiles in the postnatal rat brain. *Brain Res. Dev. Brain Res.* **145**, 117–139
75. Rebouças, E. C., Leal, S., and Sá, S. I. (2016) Regulation of NPY and α-MSH expression by estradiol in the arcuate nucleus of Wistar female rats: a stereological study. *Neurol. Res.* **38**, 740–747
76. Peng, X. R., Gennemark, P., O'Mahony, G., and Bartesaghi, S. (2015) Unlock the thermogenic potential of adipose tissue: pharmacological modulation and implications for treatment of diabetes and obesity. *Front. Endocrinol. (Lausanne)* **6**, 174
77. Miao, Y., Wu, W., Dai, Y., Maneix, L., Huang, B., Warner, M., and Gustafsson, J. A. (2015) Liver X receptor β controls thyroid hormone feedback in the brain and regulates browning of subcutaneous white adipose tissue. *Proc. Natl. Acad. Sci. USA* **112**, 14006–14011
78. Fang, S., Suh, J. M., Reilly, S. M., Yu, E., Osborn, O., Lackey, D., Yoshihara, E., Perino, A., Jacinto, S., Lukasheva, Y., Atkins, A. R., Khvat, A., Schnabl, B., Yu, R. T., Brenner, D. A., Coulter, S., Liddle, C., Schoonjans, K., Olefsky, J. M., Saltiel, A. R., Downes, M., and Evans, R. M. (2015) Intestinal FXR agonism promotes adipose tissue browning and reduces obesity and insulin resistance. *Nat. Med.* **21**, 159–165
79. Pedram, A., Razandi, M., Korach, K. S., Narayanan, R., Dalton, J. T., and Levin, E. R. (2013) ERβ selective agonist inhibits angiotensin-induced cardiovascular pathology in female mice. *Endocrinology* **154**, 4352–4364
80. Pedram, A., Razandi, M., Narayanan, R., Dalton, J. T., McKinsey, T. A., and Levin, E. R. (2013) Estrogen regulates histone deacetylases to prevent cardiac hypertrophy. *Mol. Biol. Cell* **24**, 3805–3818
81. Pedram, A., Razandi, M., O'Mahony, F., Lubahn, D., and Levin, E. R. (2010) Estrogen receptor-beta prevents cardiac fibrosis. *Mol. Endocrinol.* **24**, 2152–2165
82. Wang, Q., Zhang, M., Xu, M., Gu, W., Xi, Y., Qi, L., Li, B., and Wang, W. (2015) Brown adipose tissue activation is inversely related to central obesity and metabolic parameters in adult human. *PLoS One* **10**, e0123795
83. Tharp, K. M., and Stahl, A. (2015) Bioengineering beige adipose tissue therapeutics. *Front. Endocrinol. (Lausanne)* **6**, 164

Received for publication July 13, 2016.
Accepted for publication September 22, 2016.